

Interaction of Noncompetitive Inhibitors with the $\alpha 3\beta 2$ Nicotinic Acetylcholine Receptor Investigated by Affinity Chromatography and Molecular Docking

Krzysztof Jozwiak,^{*,†} Sarangan Ravichandran,[‡] Jack R. Collins,[‡] Ruin Moaddel,[§] and Irving W. Wainer[§]

Department of Chemistry, Medical University of Lublin, Staszica 6, 20-081 Lublin, Poland, Gerontology Research Center, National Institute on Aging, National Institutes of Health, 5600 Nathan Shock Drive, Baltimore, Maryland 21224, and Advanced Biomedical Computing Center, National Cancer Institute-Frederick/SAIC, Post Office Box B, Building 430, Miller Drive, Frederick, Maryland 21702

Received July 1, 2007

A molecular model of the $\alpha 3\beta 2$ nAChR lumen channel was constructed and hydrophobic clefts were observed near the receptor gate. Docking simulations indicated that ligand–nAChR complexes were formed by hydrophobic interactions with the cleft and hydrogen bond interactions. The equilibrium constants and association and dissociation constant rates associated with the binding interactions were determined using nonlinear chromatography on an immobilized $\alpha 3\beta 2$ nAChR column. The computational-chromatography approach can be used to predict and describe ligand–nAChR interactions.

Introduction

Neuronal nicotinic acetylcholine receptors (nAChRs^a) are ligand-gated ion channels composed of five transmembrane subunits oriented around a central pore. To date, 12 different neuronal subunits have been identified, 9 α -subunits ($\alpha 2$ – $\alpha 10$), and 3 β -subunits ($\beta 2$ – $\beta 4$), and these subunits combine to form a wide variety of homomeric and heteromeric subtypes.¹ Over 50 marketed drugs have been identified as noncompetitive inhibitors (NCIs) of nAChRs, and this property has been identified as the source of unwanted off-target clinical effects, as well as a possible new therapeutic approach.² The majority of known NCIs bind to the central lumen of the nAChR, at ring 15, and the ability to predict and describe binding at this site would be an aid in drug development.

We have previously reported a model of the lumen of the $\alpha 3\beta 4$ nAChR (PDB id: 2ASG), which included a defined hydrophobic cleft at ring 15 produced by steric interaction of the two isopropyl and three phenyl moieties of the V ($\alpha 3$) and F ($\beta 4$) residues that constitute ring 15V/F. Binding at this cleft fixes the position of the nonpolar part of a ligand, while the polar moieties form hydrogen bonds with vicinal serine residues in the 8S ring. However, this model is only applicable to nAChR subtypes containing $\beta 4$ subunits, as these are the only nAChRs that incorporate F residues into ring 15. All of the other subunits contain V in this position and, consequently, five isopropyl moieties (ring 15V).

There are pharmacological differences in the responses to NCI between nAChRs containing $\beta 4$ and those containing $\beta 2$ or $\beta 3$.³ Thus, the objective of the present work was to construct a model of the central lumen of the non- $\beta 4$ -subtype of nAChR, to examine the binding of NCIs and to compare the results to data obtained with the $\alpha 3\beta 4$ nAChR. The $\alpha 3\beta 2$ nAChR was chosen as it introduced the smallest number of changes in the amino acid composition of the lumen relative to the $\alpha 3\beta 4$ nAChR.

Methods

Chromatographic Experiments. The study utilized 18 commercially available compounds, Table 1, whose structures and sources have been previously described.⁴ The chromatographic studies were carried out as previously described,⁴ and a column containing membrane fragments obtained from a HEK293 cell line expressing recombinant $\alpha 3\beta 2$ nAChR ($\alpha 3\beta 2$ nAChR-IAM column) was prepared as previously reported.⁵

Nonlinear Affinity Chromatography. A detailed description of nonlinear chromatography on an $\alpha 3\beta 4$ -nAChR affinity column and its application in the investigation of NCIs of the nAChR has been previously reported.^{6,7} Four parameters (k' , k_{off} , k_{on} , and K) were derived using the Impulse Input Solution approach as described previously.⁶

Molecular Modeling. The molecular model of the $\alpha 3\beta 2$ nAChR binding domain for luminal NCIs was developed based on a previously generated model of the respective domain of the $\alpha 3\beta 4$ subtype of this receptor.⁴ The only differences in these models are associated with sequence polymorphisms in position 15 of the respective β subunits, where the $\beta 4$ subunit contained an F residue and the $\beta 2$ subunit contained a V residue. The modification of the $\alpha 3\beta 4$ model by replacing this residue in each $\beta 4$ M2 helix was performed with SYBYL 6.8 (Tripos Inc., St. Louis, MO). The resulted heteropentameric channel with $\alpha 3$, $\beta 2$, $\alpha 3$, $\beta 2$, and $\beta 2$ helices, respectively, was further refined by energy minimization and employed in docking simulations using AutoDock (3.0.5.), where all settings and procedures were kept the same as those used in the study of the $\alpha 3\beta 4$ nAChR.⁴

Results

Chromatographic Data. The chromatographic retentions (k') and peak profiles of the 18 test compounds were determined on the $\alpha 3\beta 2$ nAChR-IAM column. The observed k' values ranged from 4.6 (**5**) to 44.1 (**9**) and 66.3 (**3**), Table 1. In the test set, 17 of the 18 compounds have been identified as interacting with the central lumen of the nAChR. Ethidium, compound **3**, has been shown to inhibit nAChR activity through binding at a site located in the outer vestibule of the receptor and not within the central lumen.⁸ This was reflected in a retention profile that substantially differed from the other NCIs used in this study. This result was consistent with data from the previous study of binding to the $\alpha 3\beta 4$ nAChR central lumen,⁴ and, as in the previous study, the data obtained using **3** was not utilized in the further analyses.

The remaining set of 17 compounds had also been previously chromatographed on a column containing membrane fragments

* To whom correspondence should be addressed. Krzysztof Jozwiak, PhD, Department of Chemistry, Medical University of Lublin, Staszica 6, 20-081 Lublin, Poland. Tel.: +4881 5324875. Fax: +4881 5320413. E-mail: krzysztof.jozwiak@am.lublin.pl.

[†] Medical University of Lublin.

[‡] National Cancer Institute-Frederick/SAIC.

[§] National Institute on Aging, National Institutes of Health.

^a Abbreviations: nAChR, nicotinic acetylcholine receptor; NCI, non-competitive inhibitors; IAM, immobilized artificial membrane stationary phase.

Table 1. Nonlinear Chromatography (NLC) Data for All Tested Compounds and the Quantitative Results of Docking Simulations^a

compd	NLC data				docking simulations		
	<i>k'</i>	<i>k</i> _{off} [s ⁻¹]	<i>K</i> [μM ⁻¹]	<i>k</i> _{on} [μM ⁻¹ s ⁻¹]	Δ <i>G</i> [kcal/mol]	<i>K</i> _i [M ⁻¹]	
1	amantadine	5.4	24.78	1.1	26.5	-6.37	2.14 × 10 ⁻⁵
2	bupropion	10.5	15.48	1.6	25.4	-5.62	7.63 × 10 ⁻⁵
3	ethidium	66.3	1.61	22.3	35.8		
4	ketamine	6.0	23.73	0.9	21.7	-5.68	6.81 × 10 ⁻⁵
5	norketamine	4.6	27.36	0.9	24.5	-5.91	4.67 × 10 ⁻⁵
6	laudanosine	19.0	7.64	3.9	29.6	-7.26	4.75 × 10 ⁻⁶
7	mecamylamine	5.9	21.06	1.1	23.4	-5.84	5.20 × 10 ⁻⁵
8	memantine	13.1	12.56	1.9	24.2	-6.18	2.96 × 10 ⁻⁵
9	methadone	44.1	3.68	7.9	28.9	-5.75	6.14 × 10 ⁻⁵
10	methamphetamine	4.9	27.52	1.1	29.3	-4.78	3.16 × 10 ⁻⁴
11	MK-801	14.2	10.96	2.0	22.1	-6.68	1.28 × 10 ⁻⁵
12	phencyclidine	18.6	6.53	3.8	24.9	-6.52	1.66 × 10 ⁻⁵
13	(+)-3-methoxymorphinan	36.2	4.76	5.5	26.2	-7.14	5.86 × 10 ⁻⁶
14	(+)-3-hydroxymorphinan	16.2	9.39	2.3	21.2	-7.64	2.53 × 10 ⁻⁶
15	dextromethorphan	39.6	3.63	7.1	25.8	-7.60	2.69 × 10 ⁻⁶
16	dextrorphan	19.2	6.49	2.9	19.0	-7.62	2.60 × 10 ⁻⁶
17	levomethorphan	38.8	3.62	7.0	25.4	-7.26	4.76 × 10 ⁻⁶
18	levorphanol	19.3	7.58	3.2	24.1	-7.05	6.79 × 10 ⁻⁶

^a NLC data were obtained using the α3β2 nAChR column, and the quantitative results of the docking simulations (estimated free energy of interactions (Δ*G*) and estimated inhibition constant (*K*_i)) were obtained using the α3β2 nAChR subtype model.

obtained from a HEK293 cell line expressing recombinant α3β4 nAChR (α3β4 nAChR-IAM column).⁴ For 15 of the 18 compounds, the *k'* values observed on the α3β2 nAChR-IAM column were less than the *k'* values obtained on the α3β4 nAChR-IAM column, and equivalent *k'* values were observed for **5**, **9**, and **17**. The *k'* values obtained on the two nAChR subtype columns were compared using standard linear regression analysis and significant correlation was observed between the two data sets

$$k'_{(\alpha3\beta2)} = 0.736 \times k'_{(\alpha3\beta4)} + 0.623$$

$$r = 0.9325, F = 99.96, n = 17 \quad (1)$$

Retention on an affinity column is an experimental estimation of relative affinities of compounds for the immobilized selector. Thus, the results indicate that the binding affinities of the ligands to the α3β2 nAChR-IAM were significantly weaker than those observed for the α3β4 nAChR-IAM.

Chromatographic retention is the summation of specific and nonspecific interactions between the solute and the stationary phase. In both systems, HEK 293 cells were used to express the nAChR, and approximately the same number of cells was utilized to prepare the columns. Thus, it is unlikely that nonspecific interactions with the membrane fragments would be the source of the observed intercolumn differences in the *k'* values. However, if nonspecific interactions based upon lipophilic interaction played a dominant role in the overall retention, *k'* should correlate with log *P* values. The contribution of nonspecific interactions to *k'* was assessed by linear regression analysis of the *k'* and log *P* values for the 17 compounds used in the study, and no significant correlations were observed, *r*² = 0.403. Thus, on the α3β2 nAChR-IAM column, nonspecific interactions based upon lipophilicity do not play a dominant role in chromatographic retention.

Asymmetric peak shapes with excessive tailing were observed in the chromatographic traces of all of the compounds chromatographed on the α3β2 nAChR-IAM. The traces were analyzed using NLC modeling, and the resulting kinetic parameters, dissociation rate constant (*k*_{off}), association rate constant (*k*_{on}), and the equilibrium constant for adsorption (*K*) were determined, Table 1. The same analyses had been previously performed using the chromatographic traces produced by these compounds on an α3β4 nAChR-IAM.⁴

In general, the peak profiles obtained on the α3β2 nAChR-IAM column were narrower and less asymmetric than profiles obtained on the α3β4 nAChR-IAM column. According to NLC theory,⁹ peak tailing influences the *k*_{off} value and peak asymmetry, the *K* value. The comparison of *k*_{off} and *K* values obtained in two systems shows that chromatographically determined dissociation kinetics were faster in the α3β2 nAChR-IAM column and the *K* values were higher.

Previous studies with the α3β4 nAChR-IAM column have demonstrated that the *k*_{off} value is related to the stability, expressed as Δ*G*, of the NCI-nAChR complex.⁴ This was illustrated by the enantioselective differences in the *k* values of **15** and **17**, which was the result of a ΔΔ*G*^o of -0.29 kcal/mol derived from Δ*G*^o (**15**) - Δ*G*^o (**17**).⁷ Thus, it is reasonable to assume that the lower *k'* and *K* values and the higher *k*_{off} observed on the α3β2 nAChR-IAM column relative to the α3β4 nAChR-IAM reflect a reduced stability of the NCI-α3β2 nAChR complexes relative to those formed with the α3β4 nAChR-IAM.

Molecular Modeling. In the final model of the lumen of the α3β2 nAChR, the five M2 helices that comprise the binding site are oriented in a 5-fold pseudo-symmetrical manner and form a funnel-like architecture with a wide opening on the N-terminal side, Figure 1a. As has been previously described for other nAChR subtypes, there are seven rings of specific amino acids distributed along the channel, a polar ring (22 E/K) at the extracellular edge of the membrane is followed by three nonpolar rings (18 L, 15 V, 11 L) and then three polar rings (8 S, 4 T, 1E), Figure 1b. Each ring contains five residues, one from each of the five M2 helices.

In the α3β2 nAChR model, hydrophobic clefts were observed in the surface of the lumen formed by the five isopropyl moieties at 15V. The existence of these clefts was consistent with the clefts observed in the model of the α3β4 nAChR. However, the substitution of F residues in the β4 subunit by V residues in the β2 subunit produced significant differences in these areas. In the α3β2 nAChR, the packing of five isopropyl moieties into the narrow portion of the lumen produced hydrophobic clefts, which were shallow depressions (~3 Å deep) with wide round openings (~9 Å wide), Figure 2. In the α3β4 nAChR model, the steric packing produced by the presence of three phenyl

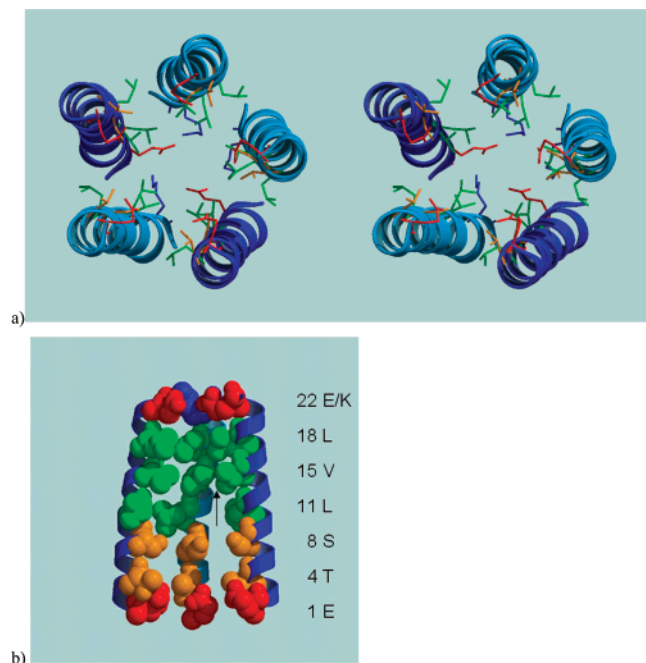


Figure 1. Graphical representation of the model of the luminal domain of the $\alpha 3\beta 2$ subtype of nAChR. The M2 helices contributed by the $\alpha 3$ subunit are colored in blue and the helices contributed by the $\beta 2$ subunit are colored in cyan. The residues lining the lumen of the channel are shown explicitly. Charged residues are shown in red and blue. Hydrophobic residues are shown in green. Hydrophilic residues are shown in orange. (a) Top view in the stereo mode (intracellular side), with exposed residues rendered in wireframe mode; and (b) side view of the channel with $\alpha 3$, $\beta 2$, and $\alpha 3$ helices shown from left to right. Two $\beta 2$ helices are removed for clarity. Exposed residues are rendered in CPK mode. Labels show the numbering of rings according to the previously reported convention.³ An arrow indicates the location of the hydrophobic cleft. The figure was prepared with MolScript v. 2.1.2¹⁴ and Raster 3D v. 2.5c.¹⁵

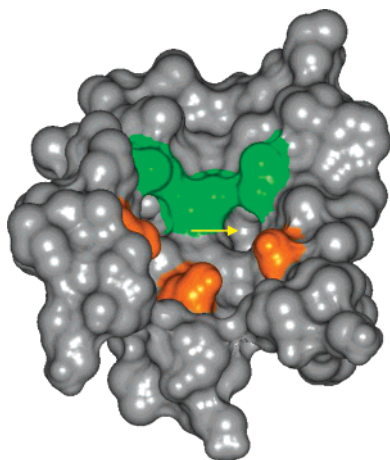


Figure 2. Hydrophobic cleft in the central lumen of the $\alpha 3\beta 2$ nAChR model developed in this study. The molecular surface (InsightII, Accelrys, Inc.) of three M2 helices (incorporated by $\alpha 3$, respective $\beta 2$ and $\alpha 3$ subunits) are shown and two helices incorporated by respective β subunits were removed. The serine residues forming the 8S ring are colored orange and residues forming the 15V ring ($\alpha 3\beta 2$) and 15V/F ring ($\alpha 3\beta 4$) are colored green (V) or blue (F). The location of the cleft is indicated by the yellow arrow.

groups resulted in the formation of a deep (~ 6 Å) and oblong pocket (~ 5 Å).⁴

Docking Simulations. Docking simulations were performed for 17 of the 18 test compounds (**3** had been removed from the set as discussed above). The AutoDock 3.0.5¹⁰ program was

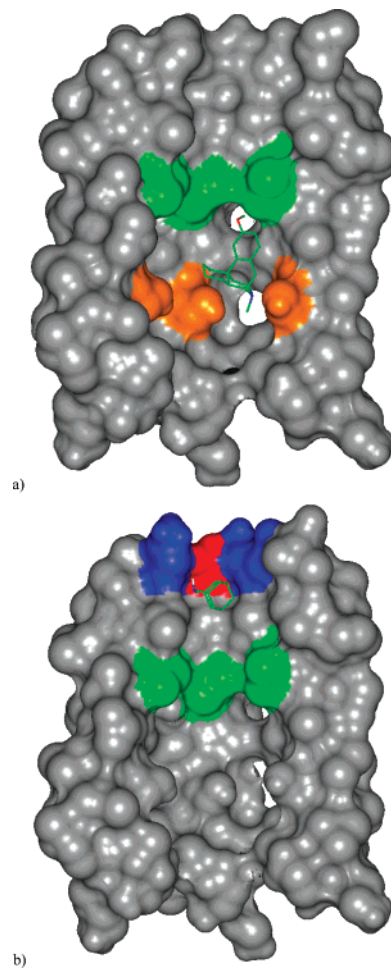


Figure 3. Lowest energy complexes of the NCI molecule with the $\alpha 3\beta 2$ nAChR lumen generated in the docking simulation. (a) The **15**– $\alpha 3\beta 2$ nAChR complex, where the lumen (side view) is rendered as a molecular surface (InsightII, Accelrys, Inc.), with the residues forming the 15V ring colored green and the 8S colored orange; the nitrogen atom of **15** can form a hydrogen bond with the S of $\beta 2$ subunit (the 8S ring). (b) The **1**– $\alpha 3\beta 2$ nAChR complex, the lumen rendered as a molecular surface, with the residues forming the 15V ring colored green and residues forming 1E/K ring colored blue (K) and red (E); the carboxyl group of E of the $\alpha 3$ subunit (the 22E/K ring) forms a hydrogen bond with the amine moiety of **1**. Ligands are rendered in stick mode with atom type color coding.

employed to determine possible orientations of the NCI molecule within the space of the internal surface of the $\alpha 3\beta 2$ channel. The modified genetic algorithm was used to generate 50 low energy conformations of the ligand–receptor complex and the default AutoDock scoring function was used to rank them and determine the lowest energy orientation.

In general, the lowest energy complexes between the tested molecules and the $\alpha 3\beta 2$ nAChR model occurred in the area between 15V and 8S, the boundary between the hydrophilic portion of the lumen (1E, 4T, and 8S) and its lipophilic portion (11L, 15V, and 18L). The complexes were formed by hydrophobic interactions with the clefts at the 15V ring and hydrogen bond interactions between polar moieties of the ligand and the 8S residues, compare Figure 3a. This binding pattern is consistent with the previously reported mechanism for NCI binding in the central lumen of the $\alpha 3\beta 4$ nAChR.⁴

Three of the tested ligands, **1**, **7**, and **8**, had different orientations in their lowest energy complexes. These ligands were bound in the region close to the extracellular entrance of the transmembrane lumen. The molecules are small enough to

penetrate through the ring 18L and form polar interactions with the glutamic acid residue of the 22E/K ring, as illustrated in Figure 3b. A similar orientation was not observed in docking studies utilizing the $\alpha 3\beta 4$ nAChR model, as the bulky phenyl rings at the 15V/F ring restricted the space in the lumen, thereby preventing ligand interactions with the 18L and 22E/K rings.

The lowest energy ligand- $\alpha 3\beta 2$ nAChR complexes were quantitatively characterized using estimated free energy of binding (ΔG , assessed by the AutoDock scoring function) and estimated inhibition constant (K_i), Table 1. When this data was compared to the ΔG values obtained from docking simulations with the $\alpha 3\beta 4$ nAChR model, the observed free energies of binding were higher for the $\alpha 3\beta 2$ nAChR than those observed for the $\alpha 3\beta 4$ nAChR, except for **1**, where the ΔG value was significantly lower. This difference may be due to the fact that, in the $\alpha 3\beta 2$ nAChR model, **1** bound closer to the top of the $\alpha 3\beta 2$ nAChR channel near the E/K ring (Figure 3b), while in the $\alpha 3\beta 4$ nAChR model, **1** could not gain access to this area.

The regression analysis demonstrated a correlation between ΔG values obtained in docking simulations on two subtypes models for the 17 ligands

$$\Delta G_{(\alpha 3\beta 2)} = 0.74 \times \Delta G_{(\alpha 3\beta 4)} - 1.20$$

$$r = 0.8708, F = 47.054, n = 17 \quad (2)$$

Discussion

The results of these studies indicate that 14 of the NCIs utilized in this investigation formed the most stable complexes within the central lumen of the $\alpha 3\beta 2$ nAChR at the 15V ring and that these complexes involved interactions with a hydrophobic cleft located at that ring. The existence of this cleft and its involvement in the formation of NCI-nAChR complexes is consistent with results from the previous studies of the $\alpha 3\beta 4$ nAChR.⁴ Thus, both nAChR subtypes interact with central-lumen binding NCIs in the same manner, and any observed differences should be quantitative not qualitative. The data from the chromatographic studies and docking studies with the $\alpha 3\beta 2$ nAChR support this assumption, as there were significant correlations with the previously reported results from studies involving the $\alpha 3\beta 4$ nAChR.

The results from the chromatographic and docking studies also indicate that the NCI-nAChR complexes formed with the $\alpha 3\beta 2$ nAChR are less stable than those formed with the $\alpha 3\beta 4$ nAChR. The major source of this difference appears to be the hydrophobic cleft, where the shallow and wide depressions in the $\alpha 3\beta 2$ nAChR model produce a less-stable complex than the clearly defined narrower and deeper cleft in the $\alpha 3\beta 4$ nAChR model.⁴

The opening of the hydrophobic gate at ring 15 of nAChRs is the result of agonist-induced conformational changes in the central lumen of the receptor,¹¹ which have been described as an organized and sequential movement of segments of the protein.¹² Previous studies in this laboratory^{4,5} have suggested that NCIs that bind in the central lumen act as a wedge and essentially freeze the nAChR central lumen in a closed conformation. The source of the inhibitory effect is the increased stability of the NCI-nAChR complex, which, in turn, increases the energies of activation required to produce the conformational changes required for the gating process.

This mechanism suggests that the model-derived reduced stabilities of the NCI- $\alpha 3\beta 2$ nAChR complexes relative to the NCI- $\alpha 3\beta 4$ nAChR complexes should be reflected in quantitative differences in the functional inhibition of these two subtypes. This effect has been observed for the inhibition of

the $\alpha 2\beta 2$, $\alpha 2\beta 4$, $\alpha 3\beta 2$, $\alpha 3\beta 4$, $\alpha 4\beta 2$, and $\alpha 4\beta 4$ nAChR subtypes by **4** and **11**.¹¹ With each subtype, **4** and **11** functioned as noncompetitive inhibitors of the receptor, but the receptors containing the $\beta 4$ subunits were more sensitive than those containing the $\beta 2$ subunits. For example, the IC_{50} values for **4** ranged between 9.5 and 29 μM for the $\beta 4$ containing nAChRs and between 50 and 92 μM when the nAChR contained $\beta 2$ subunits.

The results of this study indicate that the hydrophobic cleft at the ring 15 is present in nAChRs containing either $\beta 4$ or $\beta 2$ subunits and that these clefts play a role in the antagonist activity of NCIs. The data also indicate that chromatographic retention on the immobilized nAChR affinity column and ΔG values obtained from docking simulations can be used to screen for NCI activities and to determine relative intersubtype activity. The approach can also be used to verify if the test molecule binds at the 15V ring or, in the case of the $\alpha 3\beta 2$ nAChR, at the 18L and 22E/K rings. In addition, the data also indicate that NCIs that do not bind within the noncentral lumen, for example, **3**, can be identified using this chromatographic-bioinformatic technique, which is also consistent with previously reported results.¹³

$\alpha 3\beta 2$ nAChR and $\alpha 3\beta 4$ nAChR central lumen models represent two types of the NCI binding sites, which can be used to describe allosteric ligand interactions for the whole array of heteromeric neuronal nAChR. The $\alpha 3\beta 2$ model represents the more general model of central lumen than $\alpha 3\beta 4$, the latter can only be applicable to the $\beta 4$ -containing subtypes.

Acknowledgment. This work was supported in part by funds from the Intramural Research Program of the National Institute on Aging, NIH and the Foundation for Polish Science (FOCUS 4/2006).

References

- (1) Alexander, S. P.; Mathie, A.; Peters, J. A. Guide to receptors and channels, 1st edition (2005 revision). *Br. J. Pharmacol.* **2005**, *144* (Suppl 1), S1–128.
- (2) Moaddel, R.; Jozwiak, K.; Wainer, I. W. Allosteric modifiers of neuronal nicotinic acetylcholine receptors: new methods, new opportunities. *Med. Res. Rev.* **2007**, *27*, 723–753.
- (3) Arias, H. R.; McCardy, E. A.; Bayer, E. Z.; Gallagher, M. J.; Blanton, M. P. Allosterically linked noncompetitive antagonist binding sites in the resting nicotinic acetylcholine receptor ion channel. *Arch. Biochem. Biophys.* **2002**, *403*, 121–131.
- (4) Jozwiak, K.; Ravichandran, S.; Collins, J. R.; Wainer, I. W. Interaction of noncompetitive inhibitors with an immobilized alpha3beta4 nicotinic acetylcholine receptor investigated by affinity chromatography, quantitative-structure activity relationship analysis, and molecular docking. *J. Med. Chem.* **2004**, *47*, 4008–4021.
- (5) Moaddel, R.; Jozwiak, K.; Whittington, K.; Wainer, I. W. Conformational mobility of immobilized alpha3beta2, alpha3beta4, alpha4beta2, and alpha4beta4 nicotinic acetylcholine receptors. *Anal. Chem.* **2005**, *77*, 895–901.
- (6) Jozwiak, K.; Haginaka, J.; Moaddel, R.; Wainer, I. W. Displacement and nonlinear chromatographic techniques in the investigation of interaction of noncompetitive inhibitors with an immobilized alpha3beta4 nicotinic acetylcholine receptor liquid chromatographic stationary phase. *Anal. Chem.* **2002**, *74*, 4618–4624.
- (7) Jozwiak, K.; Hernandez, S. C.; Kellar, K. J.; Wainer, I. W. Enantioselective interactions of dextromethorphan and levomethorphan with the alpha 3 beta 4-nicotinic acetylcholine receptor: comparison of chromatographic and functional data. *J. Chromatogr., B: Biomed. Sci. Appl.* **2003**, *797*, 373–379.
- (8) Arias, H. R. Binding sites for exogenous and endogenous non-competitive inhibitors of the nicotinic acetylcholine receptor. *Biochim. Biophys. Acta* **1998**, *1376*, 173–220.
- (9) Wade, J. L.; Bergold, A. F.; Carr, P. W. Theoretical description of nonlinear chromatography, with applications to physicochemical measurements in affinity chromatography and implications for preparative-scale separations. *Anal. Chem.* **1987**, *59*, 1286–1295.

- (10) Morris, G. M.; Goodsell, D. S.; Halliday, R. S.; Huey, R.; Hart, W. E.; Belew, R. K.; Olson, A. J. Automated docking using a Lamarckian genetic algorithm and empirical binding free energy function. *J. Comput. Chem.* **1998**, *19*, 1639–1662.
- (11) Yamakura, T.; Chavez-Noriega, L. E.; Harris, R. A. Subunit-dependent inhibition of human neuronal nicotinic acetylcholine receptors and other ligand-gated ion channels by dissociative anesthetics ketamine and dizocilpine. *Anesthesiology* **2000**, *92*, 1144–1153.
- (12) Auerbach, A. Life at the top: The transition state of AChR gating. *Sci. STKE* **2003**, *2003*, re11.
- (13) Jozwiak, K.; Moaddel, R.; Yamaguchi, R.; Maciuk, A.; Wainer, I. W. Non-competitive inhibitory activities of morphinan and morphine derivatives at the alpha 3 beta 4 Neuronal nicotinic acetylcholine receptor determined using nonlinear chromatography and chemometric techniques. *Pharm. Res.* **2006**, *23*, 2175–2182.
- (14) Kraulis, P. J. MOLSCRIPT: a program to produce both detailed and schematic plots of protein structures. *J. Appl. Cryst.* **1991**, *24*, 946–950.
- (15) Merritt, E. A.; Bacon, D. J. Raster3D: Photorealistic molecular graphics. *Methods Enzymol.* **1997**, *277*, 505–524.

JM070784S